

# Decay rates for a transversely isotropic piezoelectric hollow circular nanocolumn

E Pan<sup>1\*</sup>, X Wang<sup>1</sup>, and J D Albrecht<sup>2</sup>

<sup>1</sup>Department of Civil Engineering, University of Akron, Akron, OH, USA

<sup>2</sup>Air Force Research Laboratory, Wright-Patterson Air Force Base, OH, USA

*The manuscript was received on 28 April 2007 and was accepted after revision for publication on 21 August 2007.*

DOI: 10.1243/03093247JSA324

**Abstract:** The decay rate of the elastic and electric fields along the growth direction of a transversely isotropic piezoelectric hollow or solid circular nanocolumn is investigated by developing the general solution for the corresponding three-dimensional problems. While the proposed method can be applied to asymmetric deformation, only axisymmetric deformation is considered in this paper. The derived results are first verified by comparison with existing elastic isotropic solutions. Then, the locus of smaller roots is plotted for different wall thicknesses, including also the limiting solid circular nanocolumn case. Owing to the material anisotropy and the coupling between the mechanical and electric fields, there exists an intriguing interaction of real and complex root loci for the torsionless axisymmetric deformation. The numerical results also show that the geometric parameter, material anisotropy, and piezoelectricity of the hollow or solid nanocolumn can substantially influence the decay rates, which can be applied to the strain relaxation analysis in novel semiconductor structures containing self-assembled nanoposts and nanocolumns.

**Keywords:** nanocolumn, decay rate, Saint-Venant's principle, transverse isotropy, piezoelectricity, circular cylinder, three-dimensional elasticity solution

## 1 INTRODUCTION

The decay rate of stresses and displacements along the longitudinal direction due to self-equilibrating loads acting at the end of the hollow or solid circular cylinder is an old but challenging mechanics problem. By employing the Love displacement solution, Klemm and Little [1] presented a complete analysis for a long solid circular cylinder with one end being traction free and the other end under a self-equilibrated traction. Earlier investigators on the decay of the elastic field along solid circular cylinders include Purse (see reference [2]) who obtained the eigenfunctions governing axisymmetric torsion problem, and Little and Childs [3] who obtained a vector bi-orthogonality from Love's strain function. Later, Stephen and Wang [4] considered the self-equilibrated end load

problem for a semi-infinite hollow circular cylinder by using the Papkovitch–Neuber solution to the elastostatic displacement equations of equilibrium and derived solutions for both the axisymmetric and the asymmetric cases. Stephen [5] further considered the decay rates for a compound circular cylinder of two materials having different stiffnesses. Ye [6, 7] studied the decay rates of angle-ply laminated hollow cylinders based on the recursive and approximation technique. Piezoelectric materials and structures have attracted great attention because of their capability for converting the mechanical energy into electric energy, and vice versa. As such, the corresponding Saint-Venant's principle in piezoelectricity has been investigated by many researchers (see, for example, reference [8]). These include decay rates under anti-plane [9] and plane [10, 11] deformations. However, to the best of the present authors' knowledge, the decay rate in a three-dimensional piezoelectric hollow or solid cylinder has not been studied so far, which yet may have great technical applications to the semiconductor industry, as discussed below.

\*Corresponding author: Department of Civil Engineering, University of Akron, Akron, OH, 44325-3905, USA. email: pan2@uakron.edu

In recent years, various semiconductor nanostructures have been successfully grown to enhance optoelectronic and electronic properties. Among these, the novel nanopost and nanocolumn structures are particularly of promise, as reported by Chen *et al.* [12], Van Nostrand *et al.* [13], and Thillozen *et al.* [14]. However, the strain relaxation feature along the nanopost or nanocolumn is critical from the device design point of view. Therefore, in this paper, the exact decay rates of the elastic and electric fields along the growth direction of a piezoelectric hollow or solid nanocolumn are determined by developing the general solution for the corresponding three-dimensional problems [15, 16]. While the more general asymmetric case can be discussed by using the present formulation, attention is confined to the torsional and torsionless axisymmetric cases. The numerical results presented clearly show the importance of the material anisotropy and electromechanical coupling on the decay rate of nanocolumns.

**2 GENERAL SOLUTIONS OF TRANSVERSELY ISOTROPIC PIEZOELECTRIC SOLIDS**

As shown in Fig. 1, a fixed Cartesian coordinate system ( $x, y, z$ ) and a circular cylindrical coordinate system ( $r, \theta, z$ ) are attached to the nanocolumn which is free standing on a substrate (see, for example, reference [13]). For the transversely isotropic (or hexagonal crystal) piezoelectric hollow or solid circular nanocolumn with poling direction along the  $z$  axis, the

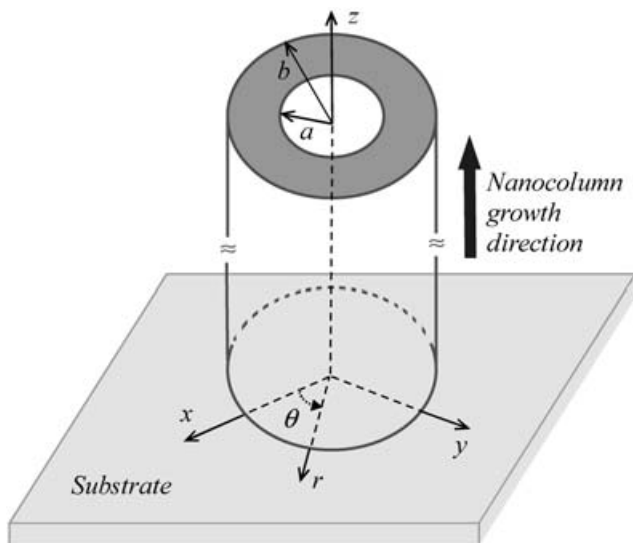


**Fig. 1** A simplified free-standing transversely isotropic piezoelectric nanocolumn over a substrate

equilibrium equations in terms of the electric potential  $\phi$  and the three displacements  $u, v$  and  $w$  along the  $x, y$  and  $z$  directions respectively are (assuming also zero body force and zero electric charge density)

$$\begin{aligned}
 &c_{11}u_{,xx} + \frac{1}{2}(c_{11} - c_{12})u_{,yy} + c_{44}u_{,zz} + \frac{1}{2}(c_{11} + c_{12})v_{,xy} \\
 &\quad + (c_{13} + c_{44})w_{,xz} + (e_{15} + e_{31})\phi_{,xz} = 0 \\
 &\frac{1}{2}(c_{11} - c_{12})v_{,xx} + c_{11}v_{,yy} + c_{44}v_{,zz} + \frac{1}{2}(c_{11} + c_{12})u_{,xy} \\
 &\quad + (c_{13} + c_{44})w_{,yz} + (e_{31} + e_{15})\phi_{,yz} = 0 \\
 &c_{44}(w_{,xx} + w_{,yy}) + c_{33}w_{,zz} + (c_{13} + c_{44})(u_{,xz} + v_{,yz}) \\
 &\quad + e_{15}(\phi_{,xx} + \phi_{,yy}) + e_{33}\phi_{,zz} = 0 \\
 &e_{15}(w_{,xx} + w_{,yy}) + e_{33}w_{,zz} + (e_{15} + e_{31})(u_{,xz} + v_{,yz}) \\
 &\quad - \varepsilon_{11}(\phi_{,xx} + \phi_{,yy}) - \varepsilon_{33}\phi_{,zz} = 0
 \end{aligned} \tag{1}$$

where  $c_{ij}, e_{ij}$ , and  $\varepsilon_{ij}$  are the elastic, piezoelectric, and dielectric coefficients respectively, of the piezoelectric solid, and the symbol  $u_{,xy}$  denotes differentiations of the elastic displacement component  $u$  with respect to  $x$  and  $y$ . In addition the linear constitutive equations in the Cartesian coordinate system are given by

$$\begin{bmatrix} \sigma_{xx} \\ \sigma_{yy} \\ \sigma_{zz} \\ \sigma_{zy} \\ \sigma_{zx} \\ \sigma_{xy} \\ D_x \\ D_y \\ D_z \end{bmatrix} = \begin{bmatrix} c_{11} & c_{12} & c_{13} & 0 & 0 & 0 & 0 & 0 & e_{31} \\ c_{12} & c_{11} & c_{13} & 0 & 0 & 0 & 0 & 0 & e_{31} \\ c_{13} & c_{13} & c_{33} & 0 & 0 & 0 & 0 & 0 & e_{33} \\ 0 & 0 & 0 & c_{44} & 0 & 0 & 0 & e_{15} & 0 \\ 0 & 0 & 0 & 0 & c_{44} & 0 & e_{15} & 0 & 0 \\ 0 & 0 & 0 & 0 & 0 & c_{66} & 0 & 0 & 0 \\ 0 & 0 & 0 & 0 & e_{15} & 0 & -\varepsilon_{11} & 0 & 0 \\ 0 & 0 & 0 & e_{15} & 0 & 0 & 0 & -\varepsilon_{11} & 0 \\ e_{31} & e_{31} & e_{33} & 0 & 0 & 0 & 0 & 0 & -\varepsilon_{33} \end{bmatrix} \times \begin{bmatrix} \varepsilon_{xx} \\ \varepsilon_{yy} \\ \varepsilon_{zz} \\ 2\varepsilon_{zy} \\ 2\varepsilon_{zx} \\ 2\varepsilon_{xy} \\ -E_x \\ -E_y \\ -E_z \end{bmatrix} \tag{2}$$

It is obvious that the  $x$ - $y$  plane is the isotropic plane and the elastic and piezoelectric properties

are uniform within this plane. In equation (2),  $c_{66} = \frac{1}{2}(c_{11} - c_{12})$  and

$$\begin{aligned} \varepsilon_{xx} &= u_{,x}, & \varepsilon_{yy} &= v_{,y}, & \varepsilon_{zz} &= w_{,z}, & \varepsilon_{xy} &= \frac{1}{2}(u_{,y} + v_{,x}) \\ \varepsilon_{zx} &= \frac{1}{2}(u_{,z} + w_{,x}), & \varepsilon_{zy} &= \frac{1}{2}(v_{,z} + w_{,y}) \\ E_x &= -\phi_{,x}, & E_y &= -\phi_{,y}, & E_z &= -\phi_{,z} \end{aligned} \quad (3)$$

It can be shown that the displacements  $u$ ,  $v$ , and  $w$ , the electric potential  $\phi$ , the stresses  $\sigma_{xx}$ ,  $\sigma_{yy}$ ,  $\sigma_{xy}$ ,  $\sigma_{zz}$ ,  $\sigma_{zx}$ , and  $\sigma_{zy}$ , and the electric displacements  $D_x$ ,  $D_y$ , and  $D_z$  can all be concisely expressed in terms of a  $3 \times 1$  harmonic function vector  $\mathbf{P} = [\Phi_1 \ \Phi_2 \ \Phi_3]^T$  and a scalar harmonic function  $\Phi_0$  as [16]

$$\begin{aligned} u + iv &= A(\tilde{\mathbf{J}}\mathbf{P} + i\Phi_0), & [w \ \phi]^T &= \mathbf{K}\mathbf{P}_{,z} \\ \sigma_{xx} + \sigma_{yy} &= 2(c_{66}\tilde{\mathbf{J}}\mathbf{H} - c_{44}\tilde{\mathbf{J}} - \tilde{\mathbf{I}}_0^T\mathbf{BK})\mathbf{P}_{,zz} \\ \sigma_{xx} - \sigma_{yy} + 2i\sigma_{xy} &= 2c_{66}A^2(\tilde{\mathbf{J}}\mathbf{P} + i\Phi_0) \\ \begin{bmatrix} \sigma_{zz} \\ D_z \end{bmatrix} &= \mathbf{B}(\tilde{\mathbf{I}}_0\tilde{\mathbf{J}} + \mathbf{K})\mathbf{H}\mathbf{P}_{,zz} \\ \begin{bmatrix} \sigma_{zx} + i\sigma_{zy} \\ D_x + iD_y \end{bmatrix} &= A\mathbf{B}[(\tilde{\mathbf{I}}_0\tilde{\mathbf{J}} + \mathbf{K})\mathbf{P}_{,z} + i\tilde{\mathbf{I}}_0\Phi_{0,z}] \end{aligned} \quad (4)$$

where

$$A = \frac{\partial}{\partial x} + i\frac{\partial}{\partial y}, \quad \tilde{\mathbf{J}} = [1 \ 1 \ 1], \quad \tilde{\mathbf{I}}_0 = [1 \ 0]^T \quad (5a)$$

$$\mathbf{K} = [\mathbf{k}_1 \ \mathbf{k}_2 \ \mathbf{k}_3], \quad \mathbf{H} = \text{diag}[\lambda_1 \ \lambda_2 \ \lambda_3] \quad (5b)$$

$$\mathbf{u} = \begin{bmatrix} c_{13} + c_{44} \\ e_{15} + e_{31} \end{bmatrix}, \quad \mathbf{A} = \begin{bmatrix} c_{33} & e_{33} \\ e_{33} & -\varepsilon_{33} \end{bmatrix} \quad (5c)$$

$$\mathbf{k}_i = \lambda_i(\mathbf{A} - \lambda_i\mathbf{B})^{-1}\mathbf{u} \quad (5d)$$

and  $\Phi_i$  ( $i = 0, 1, 2, 3$ ) satisfy

$$\Phi_{i,xx} + \Phi_{i,yy} + \lambda_i\Phi_{i,zz} = 0 \quad (i = 0, 1, 2, 3) \quad (6)$$

where  $\lambda_0 = c_{44}/c_{66}$  and  $\lambda_i$  ( $i = 1, 2, 3$ ) are the three roots of the cubic equation

$$a\lambda^3 + b\lambda^2 + c\lambda + d = 0 \quad (7)$$

with

$$\begin{aligned} a &= c_{11}(c_{44}\varepsilon_{11} + e_{15}^2) \\ b &= -c_{11}(c_{33}\varepsilon_{11} + c_{44}\varepsilon_{33} + 2e_{15}e_{33}) - c_{44}(c_{44}\varepsilon_{11} + e_{15}^2) \\ &\quad + \varepsilon_{11}(c_{13} + c_{44})^2 - c_{44}(e_{15} + e_{31})^2 \\ &\quad + 2e_{15}(c_{13} + c_{44})(e_{15} + e_{31}) \\ c &= c_{11}(c_{33}\varepsilon_{33} + e_{33}^2) + c_{44}(c_{33}\varepsilon_{11} + c_{44}\varepsilon_{33} + 2e_{15}e_{33}) \\ &\quad - \varepsilon_{33}(c_{13} + c_{44})^2 - 2e_{33}(c_{13} + c_{44})(e_{15} + e_{31}) \\ &\quad + c_{33}(e_{15} + e_{31})^2 \\ d &= -c_{44}(c_{33}\varepsilon_{33} + e_{33}^2) \end{aligned} \quad (8)$$

It should be mentioned that the above general solution (4) is only valid when  $\lambda_1 \neq \lambda_2 \neq \lambda_3$ . Therefore, when addressing the corresponding purely elastic isotropic material case or any other possible material cases where repeated roots occur, a small perturbation is given to the material coefficients to make the three eigenvalues unequal so that the general solution presented in this paper can still be applied with negligible errors (see, for example, reference [17]). The above general solution (4) can also be easily expressed in the cylindrical coordinate system  $(r, \theta, z)$  as

$$\begin{aligned} u_r + iu_\theta &= A_c(\tilde{\mathbf{J}}\mathbf{P} + i\Phi_0), & [w \ \phi]^T &= \mathbf{K}\mathbf{P}_{,z} \\ \sigma_{rr} + \sigma_{\theta\theta} &= 2(c_{66}\tilde{\mathbf{J}}\mathbf{H} - c_{44}\tilde{\mathbf{J}} - \tilde{\mathbf{I}}_0^T\mathbf{BK})\mathbf{P}_{,zz} \\ \sigma_{rr} - \sigma_{\theta\theta} + 2i\sigma_{r\theta} &= 2c_{66}(A_c^2 - r^{-1}A_c)(\tilde{\mathbf{J}}\mathbf{P} + i\Phi_0) \\ \begin{bmatrix} \sigma_{zz} \\ D_z \end{bmatrix} &= \mathbf{B}(\tilde{\mathbf{I}}_0\tilde{\mathbf{J}} + \mathbf{K})\mathbf{H}\mathbf{P}_{,zz} \\ \begin{bmatrix} \sigma_{zr} + i\sigma_{z\theta} \\ D_r + iD_\theta \end{bmatrix} &= A_c\mathbf{B}[(\tilde{\mathbf{I}}_0\tilde{\mathbf{J}} + \mathbf{K})\mathbf{P}_{,z} + i\tilde{\mathbf{I}}_0\Phi_{0,z}] \end{aligned} \quad (9)$$

where

$$\begin{aligned} A_c &= \frac{\partial}{\partial r} + i\frac{1}{r}\frac{\partial}{\partial \theta} \\ A_c^2 - \frac{1}{r}A_c &= \left(\frac{\partial}{\partial r} - \frac{1}{r} + i\frac{1}{r}\frac{\partial}{\partial \theta}\right)\left(\frac{\partial}{\partial r} + i\frac{1}{r}\frac{\partial}{\partial \theta}\right) \end{aligned} \quad (10)$$

For the torsional axisymmetric deformation of the piezoelectric solid,  $u_r = w = \phi = \sigma_{rr} = \sigma_{\theta\theta} = \sigma_{zz} = \sigma_{zr} = D_r = D_z = 0$  and  $\mathbf{P} = \mathbf{0}$ . Then the general solution (9)

is reduced to

$$u_\theta = \Phi_{0,r}, \quad \sigma_{r\theta} = c_{66}(\Phi_{0,rr} - r^{-1}\Phi_{0,r})$$

$$\begin{bmatrix} \sigma_{z\theta} \\ D_\theta \end{bmatrix} = \mathbf{B}\tilde{\mathbf{I}}_0 \Phi_{0,rz}$$
(11)

On the other hand, for the torsionless axisymmetric deformation of the piezoelectric solid,  $u_\theta = \sigma_{r\theta} = \sigma_{z\theta} = D_\theta = 0$  and  $\Phi_0 = 0$ . For this case, the above general solution (9) is reduced to

$$u_r = \bar{\mathbf{J}}\mathbf{P}_{,r}, \quad [w \quad \phi]^T = \mathbf{K}\mathbf{P}_{,z}$$

$$\sigma_{rr} + \sigma_{\theta\theta} = 2(c_{66}\tilde{\mathbf{J}}\mathbf{H} - c_{44}\tilde{\mathbf{J}} - \tilde{\mathbf{I}}_0^T\mathbf{B}\mathbf{K})\mathbf{P}_{,zz}$$

$$\sigma_{rr} - \sigma_{\theta\theta} = 2c_{66}\tilde{\mathbf{J}}(\mathbf{P}_{,rr} - r^{-1}\mathbf{P}_{,r})$$

$$\begin{bmatrix} \sigma_{zz} \\ D_z \end{bmatrix} = \mathbf{B}(\tilde{\mathbf{I}}_0\tilde{\mathbf{J}} + \mathbf{K})\mathbf{H}\mathbf{P}_{,zz}, \quad \begin{bmatrix} \sigma_{zr} \\ D_r \end{bmatrix} = \mathbf{B}(\tilde{\mathbf{I}}_0\tilde{\mathbf{J}} + \mathbf{K})\mathbf{P}_{,rz}$$
(12)

### 3 DECAy RATES OF THE TRANSVERSELY ISOTROPIC PIEZOELECTRIC NANOCOLUMN

It is assumed that the circular hollow nanocolumn occupies the region  $a \leq r \leq b$ ,  $0 \leq z \leq +\infty$ . In this investigation, only the torsional and torsionless axisymmetric deformations of the nanocolumn are considered. The two lateral surfaces of the column  $r = a$  and  $r = b$  are traction free; thus

$$\sigma_{rr} = \sigma_{rz} = \sigma_{r\theta} = 0, \quad \text{on } r = a \text{ and } r = b$$
(13)

In addition, either the charge-free (insulating) condition  $D_r = 0$  or electroded (conducting) condition  $\phi = 0$  is imposed on the two surfaces  $r = a$  and  $r = b$ .

#### 3.1 Torsional case

It is first pointed out that the torsional case is purely elastic and that its solution is associated with the scalar harmonic function  $\Phi_0$  only. Assuming that the field quantity in the nanocolumn decays exponentially in its growth direction, then

$$\Phi_0 = B_1 J_0(\rho\sqrt{\lambda_0}r) e^{-\rho z} + B_2 Y_0(\rho\sqrt{\lambda_0}r) e^{-\rho z}$$
(14)

where  $B_1$  and  $B_2$  are two constants to be determined, and  $J_n$  and  $Y_n$  are the  $n$ th-order Bessel functions of

the first and second kinds respectively. Substituting equation (14) into the general solution (11) and imposing the traction-free boundary conditions  $\sigma_{r\theta} = 0$  on  $r = a$  and  $r = b$ , the homogeneous linear equations for  $B_1$  and  $B_2$  are

$$\begin{bmatrix} J_2(\rho\sqrt{\lambda_0}a) & Y_2(\rho\sqrt{\lambda_0}a) \\ J_2(\rho\sqrt{\lambda_0}b) & Y_2(\rho\sqrt{\lambda_0}b) \end{bmatrix} \begin{bmatrix} B_1 \\ B_2 \end{bmatrix} = \begin{bmatrix} 0 \\ 0 \end{bmatrix}$$
(15)

A non-trivial solution for equation (15) yields the transcendental equation for  $\rho$  according to

$$J_2(\rho\sqrt{\lambda_0}a)Y_2(\rho\sqrt{\lambda_0}b) - Y_2(\rho\sqrt{\lambda_0}a)J_2(\rho\sqrt{\lambda_0}b) = 0$$
(16)

which is identical with that derived by Stephen and Wang [4] if we set  $k = \rho\sqrt{\lambda_0}$ . Therefore, once the decay rate for the torsional deformation of an isotropic elastic hollow cylinder is calculated, the torsional decay rate for the corresponding transversely isotropic piezoelectric nanocolumn can be simply found by dividing result by the factor  $\sqrt{\lambda_0}$ . In other words, the decay rate for the torsional case of the transversely isotropic piezoelectric nanocolumn is inversely proportional to the ratio  $\sqrt{\lambda_0} = \sqrt{c_{44}/c_{66}}$ .

#### 3.2 Torsionless case

Similarly, for this case, it is assumed that the physical quantity in the nanocolumn decays exponentially as

$$\mathbf{P} = e^{-\rho z} [\langle J_0(\rho\sqrt{\lambda_\alpha}r) \rangle \mathbf{C}_1 + \langle Y_0(\rho\sqrt{\lambda_\alpha}r) \rangle \mathbf{C}_2]$$
(17)

where the angular brackets  $\langle \cdot \rangle$  stand for a  $3 \times 3$  diagonal matrix with its element varying with the index  $\alpha$ , and  $\mathbf{C}_1$  and  $\mathbf{C}_2$  are two  $3 \times 1$  constant vectors to be determined. Substituting equation (17) into the general solution (12) and imposing the traction-free and charge-free (or electroded) boundary conditions on  $r = a$  and  $r = b$ , the homogeneous linear equations for  $\mathbf{C}_1$  and  $\mathbf{C}_2$  are

$$\mathbf{A}_{11}\mathbf{C}_1 + \mathbf{A}_{12}\mathbf{C}_2 = \mathbf{0}$$

$$\mathbf{A}_{21}\mathbf{C}_1 + \mathbf{A}_{22}\mathbf{C}_2 = \mathbf{0}$$
(18)

where the elements of the matrices  $\mathbf{A}_{ij}$  are given below for different boundary conditions at  $r = a$  and  $r = b$ .



The condition that equation (18) admits a non-trivial solution yields the transcendental equation for  $\rho$  as

$$\begin{vmatrix} \mathbf{A}_{11} & \mathbf{A}_{12} \\ \mathbf{A}_{21} & \mathbf{A}_{22} \end{vmatrix} = 0 \quad (23)$$

It should be noted that, when the piezoelectric tensor vanishes (i.e.  $e_{ij} = 0$ ), the problem decouples into purely elastic and purely dielectric problems. While the purely elastic case is still relative complicated, the purely dielectric case can be simply discussed below for different electric boundary conditions.

It is found that, if both  $r = a$  and  $r = b$  of a dielectric hollow circular nanocolumn are charge free, then the transcendental equation for  $\rho$  is

$$J_1(s\rho a)Y_1(s\rho b) - Y_1(s\rho a)J_1(s\rho b) = 0 \quad (24)$$

where

$$s = \sqrt{\frac{\varepsilon_{33}}{\varepsilon_{11}}} \quad (25)$$

If both  $r = a$  and  $r = b$  are electroded, then the transcendental equation for  $\rho$  is

$$J_0(s\rho a)Y_0(s\rho b) - Y_0(s\rho a)J_0(s\rho b) = 0 \quad (26)$$

If  $r = a$  is charge free while  $r = b$  is electroded, then the transcendental equation for  $\rho$  is

$$J_1(s\rho a)Y_0(s\rho b) - Y_1(s\rho a)J_0(s\rho b) = 0 \quad (27)$$

If  $r = a$  is electroded while  $r = b$  is charge free, then the transcendental equation for  $\rho$  is

$$J_0(s\rho a)Y_1(s\rho b) - Y_0(s\rho a)J_1(s\rho b) = 0 \quad (28)$$

The calculations show that the roots to the transcendental equations (24), (26), (27), and (28) are all real.

#### 4 RESULTS AND DISCUSSION

First, the results are verified by comparison with existing isotropic solutions. It is noted that, by using a small perturbation from isotropy to anisotropy, the decay rates based on the present formulation are in complete agreement with those obtained by Little and Childs [3] for an isotropic elastic solid circular cylinder, and by Stephen and Wang [4] for an isotropic elastic hollow circular cylinder. For example, in Fig. 2 the complex decay roots  $\rho b$  for axisymmetric torsionless displacements for an isotropic elastic hollow cylinder with Poisson's ratio  $\nu = 0.25$  are illustrated. It is

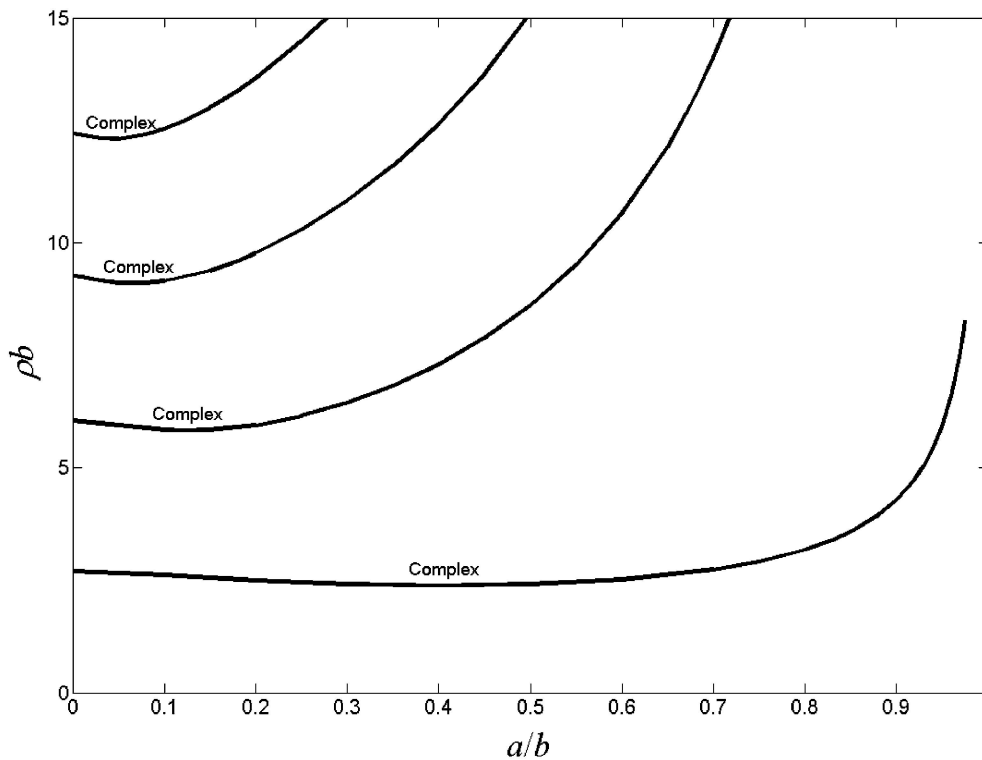


**Fig. 2** Dimensionless complex decay roots  $\rho b$  under axisymmetric torsionless deformation for an isotropic elastic hollow nanocolumn with Poisson's ratio  $\nu = 0.25$ . Only real parts of the roots are shown

observed that Fig. 2 is identical with Fig. 3 in the paper by Stephen and Wang [4].

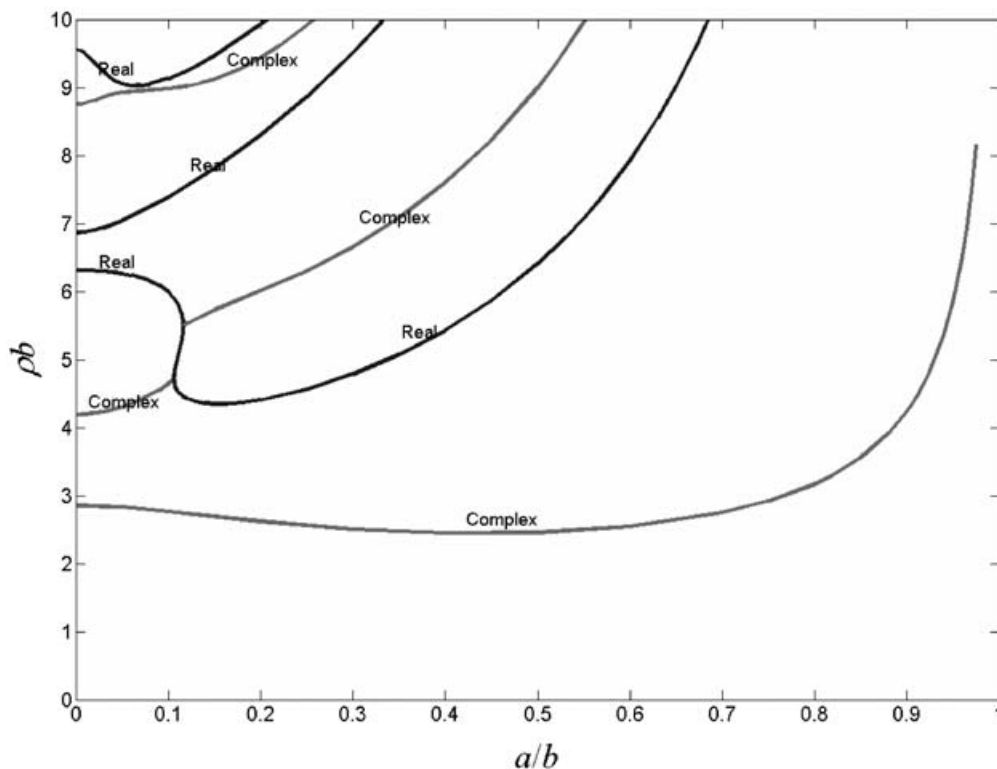
Next, the specific results for the transversely isotropic piezoelectric gallium nitride (GaN) nanocolumn [13] are presented. It is noted that GaN is a semiconductor compound with strong coupling between the electric and mechanical fields and with a wide energy bandgap [18, 19]. As such, the corresponding GaN nanopost and nanocolumn growth and overgrowth have recently attracted wide attention in the semiconductor community (see, for example, references [12] to [14]). The material properties of the transversely isotropic (or hexagonal) GaN with its material symmetry axis along the  $z$  direction are listed in Table 1.

Figure 3 demonstrates the dimensionless real and complex decay roots  $\rho b$  under the axisymmetric torsionless deformation for the transversely isotropic piezoelectric hollow GaN nanocolumn. Both surfaces  $r = a$  and  $r = b$  are insulating, i.e.  $D_r = 0$ . Similarly, Fig. 4 presents the corresponding results when both  $r = a$  and  $r = b$  are conducting (or electroded), i.e.  $\phi = 0$ . It is found that, even for the axisymmetric torsionless case, there exists an intriguing interaction between the real and complex root loci due to the

**Table 1** Material properties of GaN [18, 19]

$c_{11} = c_{22}$ (GPa)	390.0
$c_{33}$ (GPa)	398.0
$c_{12}$ (GPa)	145.0
$c_{13} = c_{23}$ (GPa)	106.0
$c_{44} = c_{55}$ (GPa)	105.0
$c_{66} = (c_{11} - c_{12})/2$ (GPa)	122.5
$e_{15}$ (C/m <sup>2</sup> )	-0.30
$e_{31}$ (C/m <sup>2</sup> )	-0.33
$e_{33}$ (C/m <sup>2</sup> )	0.65
$\epsilon_{11} = \epsilon_{22}$ ( $10^{-12}$ C <sup>2</sup> /N m <sup>2</sup> )	78.8
$\epsilon_{33}$ ( $10^{-12}$ C <sup>2</sup> /N m <sup>2</sup> )	78.8

anisotropic effect and the electromechanical coupling (the piezoelectric effect). For the purely elastic and isotropic case, such interactions only occur for the non-axisymmetric deformation [4]. Different electrical boundary conditions (insulating or conducting) also influence the root loci. The decay rate, defined as the decay distance of end effects (or the strain relaxation rate), is the real part of the root with smallest positive real part. By comparing Fig. 3 and Fig. 4, it is found that, when  $a/b > 0.05$ , the difference between the decay rates for the insulating and conducting cases is minimal. On the other hand, the discrepancy in



**Fig. 3** Dimensionless real and complex decay roots  $\rho b$  under axisymmetric torsionless deformation for a transversely isotropic piezoelectric hollow GaN nanocolumn with boundary condition  $D_r = 0$  on  $r = a$  and  $r = b$ . Only real parts of the roots are shown

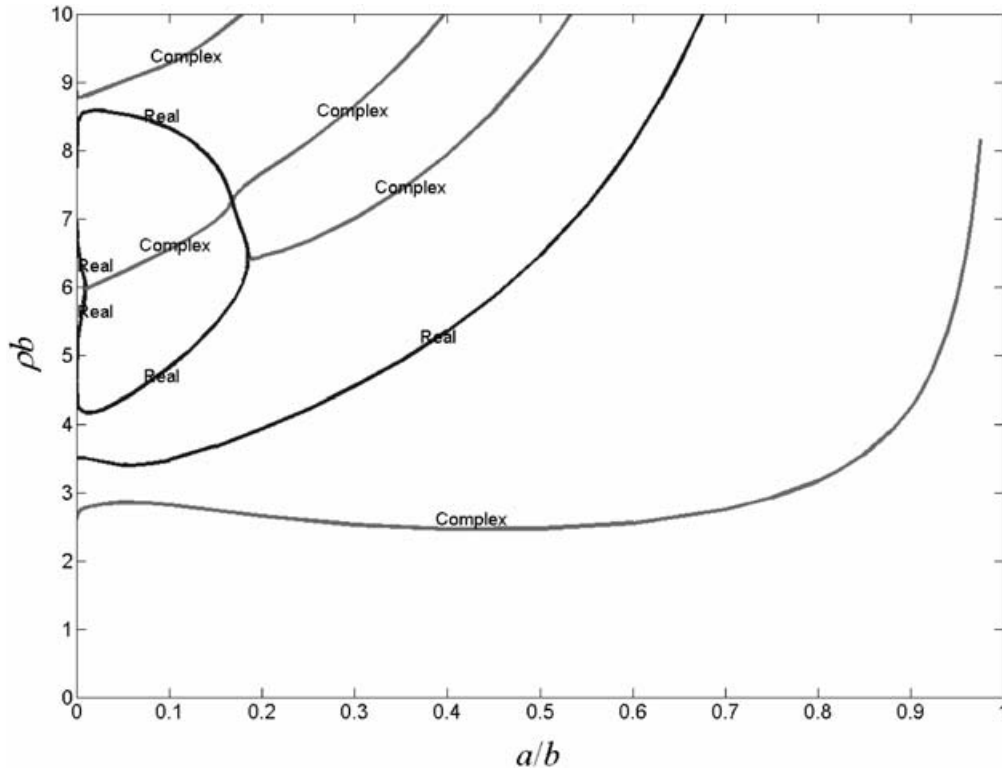


**Fig. 4** Dimensionless real and complex decay roots  $\rho b$  under axisymmetric torsionless deformation for a transversely isotropic piezoelectric hollow GaN nanocolumn with boundary condition  $\phi = 0$  on  $r = a$  and  $r = b$ . Only real parts of the roots are shown

decay rates for the two different electric conditions is most apparent for a solid cylinder:  $\rho b = 2.855$  for the insulating condition and  $\rho b = 2.605$  for the conducting condition.

It should be noted that Fig. 3 should be extremely useful for the GaN nanopost and nanocolumn growth as the experimental environment is most probably insulating instead of conducting. For instance, for a solid GaN nanocolumn of radius  $b = 100$  nm, using the normalized decay rate  $\rho b = 2.855$ , it is found that the elastic and electric fields at the height  $z = 161$  nm are reduced to 1 per cent of the value at the bottom of the nanocolumn  $z = 0$ . It is further observed from Fig. 3 that, for a hollow GaN nanocolumn, there is a special ratio  $a/b$  where the normalized decay rate reaches its minimum (i.e.  $\rho b = 2.447$  at  $a/b = 0.4$ ). When the wall of the hollow nanocolumn becomes thinner than  $a/b = 0.4$ , then the normalized decay rate increases. The thinner the hollow nanocolumn, the faster the elastic and electric fields decay.

In order to demonstrate clearly how the piezoelectricity influences the decay roots, in Fig. 5 the decay roots for a GaN hollow nanocolumn are presented by ignoring the piezoelectric effects (i.e.  $e_{ij} = 0$ ). In Fig. 5, besides the decoupled purely elastic roots under the traction-free boundary condition, the

decoupled purely electric roots under the insulating boundary condition (by the marked dashed lines) are also presented for comparison. Furthermore, in Fig. 5, the smallest decay mode loci have been redrawn (from Figs 3 and 4) for the corresponding fully coupled piezoelectric case (dashed curves for the insulating condition on the two surfaces, and dash-dotted curves for the conducting condition on the two surfaces). By comparing Fig. 5 with the previous two figures (Figs 3 and 4), it is observed that the piezoelectric effect can influence the root loci, especially those of the higher decay modes. As far as the decay rate is concerned, the piezoelectric effects must be taken into consideration for thick cylinders,  $a/b < 0.2$ , and they can only be ignored for relatively thin cylinders,  $a/b > 0.2$ . In other words, in the analysis of the strain and electric fields in GaN nanocolumn structures, it is recommended that the fully coupled piezoelectric model should be employed (see, for example, references [20] to [22]). This is particularly true for the solid nanocolumn where a decay rate of  $\rho b = 3.2213$  is predicted for the decoupled purely elastic case, and  $\rho b = 2.855$  and  $\rho b = 2.605$  correspond to the fully coupled piezoelectric case with insulating and conducting boundary conditions respectively (Fig. 5 for the

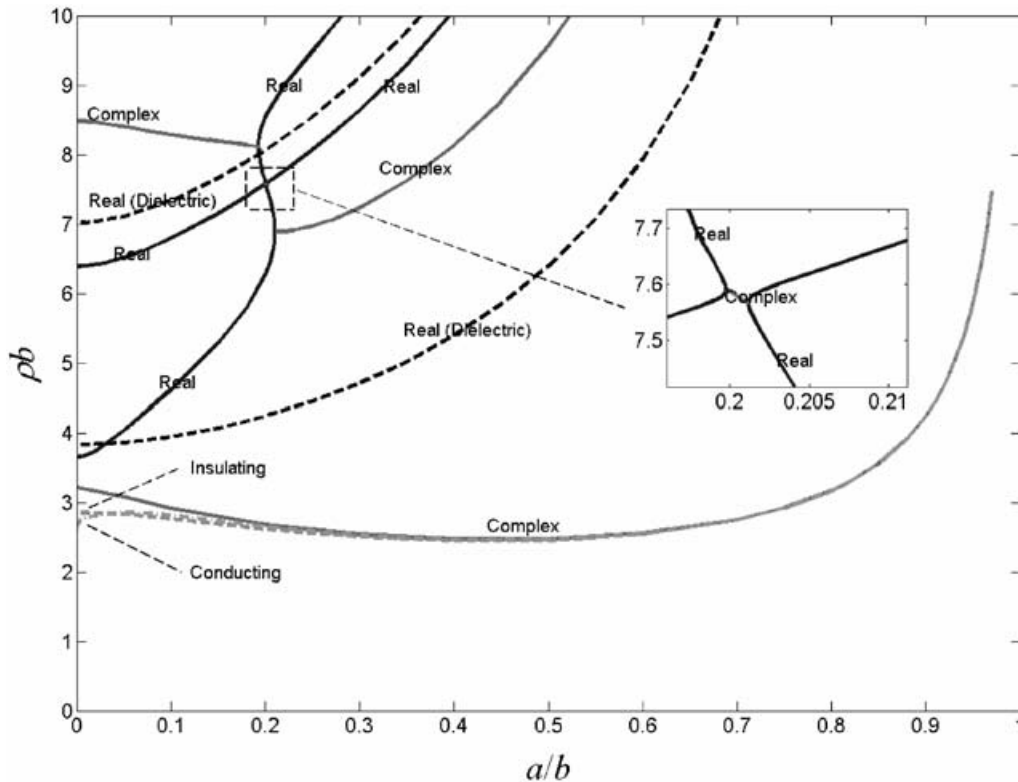


**Fig. 5** Dimensionless real and complex decay roots  $\rho b$  under axisymmetric torsionless deformation for a decoupled purely elastic and purely electric hollow GaN nanocolumn. The smallest decay model loci of the corresponding fully coupled piezoelectric case are also shown for comparison (the dashed curves are for insulating boundary conditions and the dash-dotted curves for conducting boundary conditions on the two surfaces). Only real parts of the roots are shown

smallest loci at  $a/b = 0$ ). Figure 5 also indicates clearly that, even for the decoupled piezoelectric case, an interaction between the real and complex root loci still exists. It should be mentioned that the decay roots for the axisymmetric torsionless displacements for an isotropic elastic hollow nanocolumn are all complex and there is no mode-coupling phenomenon (see Fig. 2 here or Fig. 3 in the paper by Stephen and Wang [4]). Thus it is concluded that the material anisotropy in a nanocolumn can also significantly influence the decay roots.

## 5 CONCLUSIONS

The decay rate of the elastic and piezoelectric fields along a transversely isotropic piezoelectric hollow or solid circular nanocolumn is investigated in detail by developing the general solution for the corresponding three-dimensional problem. It is shown clearly that the geometric parameter, material anisotropy, and piezoelectricity can all significantly affect the decay rate and thus can influence the strain and

electric field relaxation in the piezoelectric hollow or solid nanocolumn. In particular, a solid GaN nanocolumn can have a decay rate of  $\rho b = 3.2213$  for the decoupled purely elastic case, and  $\rho b = 2.855$  and  $\rho b = 2.605$  for the fully coupled piezoelectric case with insulating and conducting boundary conditions respectively. This obviously indicates that the piezoelectric effect cannot be ignored for a solid GaN nanocolumn as far as the decay rate is concerned. The results presented in this paper should be particularly useful to guide the nanopost and nanocolumn growth where the growth-induced strain is critical to the corresponding semiconductor nanostructured devices. Even though only the simple axisymmetric case is discussed, the methodology can be easily extended to the more complicated asymmetric case. For the asymmetric case, because of the coupling between torsional and torsionless displacements, and between mechanical and electric fields (the piezoelectric effects), and because of the anisotropic effect, it is expected that the decay root loci for this situation are more complex than their isotropic counterparts.

## ACKNOWLEDGEMENTS

This work was supported in part by Grant AFOSR FA9550-06-1-0317. The first author would also like to thank Mr Harish Gopalan for his help with the initial coding task.

## REFERENCES

- 1 Klemm, J. L. and Little, R. W. The semi-infinite elastic cylinder under self-equilibrated end loading. *SIAM J. Appl. Math.*, 1970, **19**, 712–729.
- 2 Love, A. E. H. *A treatise on the mathematical theory of elasticity*, 4th edition, 1944 (Dover Publications, New York).
- 3 Little, R. W. and Childs, S. B. Elastostatic boundary region problems on solid cylinders. *Q. Appl. Math.*, 1967, **25**, 261–274.
- 4 Stephen, N. G. and Wang, M. Z. Decay rates for the hollow circular cylinder. *Trans. ASME, J. Appl. Mechanics*, 1992, **59**, 747–753.
- 5 Stephen, N. G. Decay rates for the compound circular cylinder. *J. Strain Analysis*, 1991, **26**, 215–220.
- 6 Ye, J. Q. Edge effects in angle-ply laminated hollow cylinders. *Computers Structs*, 2001, **52**, 247–253.
- 7 Ye, J. Q. Decay rate of edge effects in cross-ply laminated hollow cylindrical shells. *Int. J. Mech. Sci.*, 2001, **43**, 455–470.
- 8 Batra, R. C. and Yang, J. S. Saint-Venant's principle in linear piezoelectricity. *J. Elasticity*, 1995, **38**, 209–218.
- 9 Borrelli, A., Horgan, C. O., and Patria, M. C. Saint-Venant end effects in anti-plane shear for classes of linear piezoelectric materials. *J. Elasticity*, 2001, **64**, 217–236.
- 10 Fan, H. Decay rates in a piezoelectric strip. *Int. J. Engng Sci.*, 1995, **33**, 1095–1103.
- 11 Borrelli, A., Horgan, C. O., and Patria, M. C. Saint-Venant end effects for plane deformations of linear piezoelectric solids. *Int. J. Solids Structs*, 2006, **43**, 943–956.
- 12 Chen, H. S., Yeh, D. M., Lu, Y. C., Chen, C. Y., Huang, C. F., Tang, T. Y., Yang, C. C., Wu, C. S., and Chen, C. D. Strain relaxation and quantum confinement in InGaN/GaN nanoposts. *Nanotechnology*, 2006, **17**, 1454–1458.
- 13 Van Nostrand, J. E., Averett, K., Cortez, R., Boeckl, J., Stutz, C. E., Sanford, N. A., Davydov, A. V., and Albrecht, J. D. Molecular beam epitaxy of high-quality GaN nanocolumns. *J. Crystal Growth*, 2006, **287**, 500–503.
- 14 Thillozen, N., Sebald, K., Hardtdegen, H., Meijers, R., Calarco, R., Montanari, S., Kaluza, N., Gutowski, J., and Luth, H. The state of strain in single GaN nanocolumns as derived from micro-photoluminescence measurements. *Nano Lett.*, 2006, **6**, 704–708.
- 15 Ding, H. J., Chen, B., and Liang, J. General solutions for coupled equations for piezoelectric media. *Int. J. Solids Structs*, 1996, **33**, 2283–2298.
- 16 Wang, X. An electric point charge moving along the poling direction of a transversely isotropic piezoelectric solid. *Arch. Appl. Mechanics*, 2005, **74**, 509–516.
- 17 Pan, E. A BEM analysis of fracture mechanics in 2-D anisotropic piezoelectric solids. *Engng Analysis Boundary Elements*, 1999, **23**, 67–76.
- 18 Levinshtein, M. E., Rumyantsev, S. L., and Shur, M. S. (Eds) *Properties of advanced semiconductor materials GaN, AlN, InN, BN, SiC, SiGe*, 2001 (John Wiley, New York).
- 19 Vurgaftman, I., Meyer, J. R., and Ram-Mohan, L. R. Band parameters for III-V compound semiconductors and their alloys. *J. Appl. Phys.*, 2001, **89**, 5815–5875.
- 20 Pan, E. Elastic and piezoelectric fields around a quantum dot: fully coupled or semi-coupled model? *J. Appl. Phys.*, 2002, **91**, 3785–3796.
- 21 Jogai, B., Albrecht, J. D., and Pan, E. The effect of electromechanical coupling on the strain in AlGaIn/GaN heterojunction field effect transistors. *J. Appl. Phys.*, 2003, **94**, 3984–3989.
- 22 Jogai, B., Albrecht, J. D., and Pan, E. Electro-mechanical coupling in free-standing AlGaIn/GaN planar structures. *J. Appl. Phys.*, 2003, **94**, 6566–6573.

## APPENDIX

## Notation

$a, b$	radii of the circular hollow
$\mathbf{A}, \mathbf{B}$	two $2 \times 2$ real and symmetric matrices
$\mathbf{A}_{ij}$	$3 \times 3$ matrix ( $i, j = 1, 2$ )
$c_{ij}, e_{ij}, \varepsilon_{ij}$	elastic, piezoelectric and dielectric coefficients respectively of the piezoelectric solid
$D_r, D_\theta$	electric displacements in the circular cylindrical system
$D_x, D_y, D_z$	electric displacements in the Cartesian coordinate system
$\mathbf{H}$	$3 \times 3$ diagonal matrix
$\tilde{\mathbf{I}}_0$	$2 \times 1$ matrix = $[1 \quad 0]^T$
$J_n, Y_n$	$n$ th-order Bessel functions of the first and second kinds respectively
$\tilde{\mathbf{J}}$	$1 \times 3$ matrix = $[1 \quad 1 \quad 1]$
$\mathbf{K}$	$2 \times 3$ matrix
$\mathbf{P}$	$3 \times 1$ harmonic function vector
$r, \theta, z$	circular cylindrical coordinates
$u, v, w$	displacement components along the $x, y,$ and $z$ directions respectively
$u_r, u_\theta$	displacement components along the $r$ and $\theta$ directions respectively
$\mathbf{u}$	$2 \times 1$ matrix
$x, y, z$	Cartesian coordinates

$A$	differential operator in the Cartesian coordinate system	$\sigma_{xx}, \sigma_{yy}, \sigma_{zz}, \sigma_{zx}, \sigma_{zy}, \sigma_{xy}$	stress components in the Cartesian coordinate system
$A_c$	differential operator in the circular cylindrical system	$\phi$	electric potential
$\sigma_{rr}, \sigma_{\theta\theta}, \sigma_{zr}, \sigma_{z\theta}, \sigma_{r\theta}$	stress components in the circular cylindrical system	$\Phi_0$	scalar harmonic function
		$[0 \ 1]$	$1 \times 2$ matrix